

Properties of the predicted super-deformed band in ^{32}S .

R. R. Rodríguez-Guzmán, J.L. Egido and L.M. Robledo

Departamento de Física Teórica C-XI, Universidad Autónoma de Madrid, 28049 Madrid, Spain.

(October 27, 2018)

Properties like the excitation energy with respect to the ground state, moments of inertia, $B(E2)$ transition probabilities and stability against quadrupole fluctuations at low spin of the predicted superdeformed band of ^{32}S are studied with the Gogny force D1S using the angular momentum projected generator coordinate method for the axially symmetric quadrupole moment. The Self Consistent Cranking method is also used to describe the superdeformed rotational band. In addition, properties of some collective normal deformed states are discussed.

21.60.Jz, 21.60.-n, 21.10.Re, 21.10.Ky, 21.10.Dr, 27.30.+t

I. INTRODUCTION.

Recently, a number of papers have addressed the theoretical study of the predicted super deformed (SD) configuration in the nucleus ^{32}S by using the mean field approximation at high spin with several flavors of the Skyrme [1,2] and also the Gogny interaction [3]. The interest to study the SD configuration in ^{32}S comes from the fact that this SD configuration is thought to be an intermediate case between the strongly deformed cluster structures in very light nuclei and the known SD states in the $A = 60$ region [4,5]. In fact, it is interesting to understand the relationship between the predicted SD band in ^{32}S and the $^{16}\text{O} + ^{16}\text{O}$ quasimolecular rotational states observed in this nucleus [6,7]. On the other hand, many states up to an excitation energy of around 10MeV are known experimentally in this nucleus [8]. Those states can be interpreted in terms of the shell model with active particles in the sd shell [9] and also in terms of the algebraic cluster model [10]. It turns out that some of these states can be interpreted in terms of deformed intrinsic configurations and, therefore, they can be used as a test ground to assure the reliability of any interaction meant to describe the SD band in this nucleus at the mean field level.

The purpose of this paper is to study, using the Gogny interaction [11] with the D1S parameterization [12], the properties of the superdeformed band of the nucleus ^{32}S focusing on the stability of the superdeformed minimum at low spin against quadrupole fluctuations. The reason is that in the theoretical studies mentioned in the above paragraph and also in previous mean field calculations with the Skyrme [13] and Gogny forces [14] the SD minimum observed in the energy landscape was very shallow rising serious doubts about its ability to hold states at low angular momentum when fluctuations in the quadrupole degree of freedom are taken into consideration (see [2] for a discussion of this issue). Obviously, at higher spins the rotational energy makes the SD minimum deeper and therefore much more stable against quadrupole fluctuations. As a side product of our calculations and also to check the suitability of the Gogny force for this nucleus we have studied the properties of low lying normal deformed states and compared them with the available experimental data. To perform the theoretical analysis, we have used the Angular Momentum Projected Generator Coordinate Method (AMP-GCM) with the axial quadrupole moment as generating coordinate and restricted ourselves to $K = 0$ configurations. The method allows to obtain an accurate estimate of the excitation energy of the superdeformed 0^+ state with respect to the ground state. The properties of the superdeformed band obtained with the AMP-GCM are also compared to those of a Self Consistent Cranking calculation. The choice of the Gogny interaction for this calculation is backed up not only by the results we obtain for low lying excited states but also by previous calculations in the context of the Bohr hamiltonian in the β and γ collective variables at zero spin for normal deformed states that were used to describe neutron and proton pair transfer reactions [15] and proton scattering [16] data with great success.

II. THEORETICAL FRAMEWORK.

In the framework of the Angular Momentum Projected Generator Coordinate Method (AMP-GCM) we have used the following ansatz for the $K = 0$ wave functions of the system

$$|\Phi_{\sigma}^I\rangle = \int dq_{20} f_{\sigma}^I(q_{20}) \hat{P}_{00}^I |\varphi(q_{20})\rangle. \quad (1)$$

In this expression $|\varphi(q_{20})\rangle$ is the set of axially symmetric (i.e. $K = 0$) Hartree-Fock-Bogoliubov (HFB) wave functions generated with the constraint $\langle\varphi(q_{20})|z^2 - 1/2(x^2 + y^2)|\varphi(q_{20})\rangle = q_{20}$ on the mass quadrupole moment. The HFB wave functions have been expanded in an axially symmetric Harmonic Oscillator (HO) basis with 10 major shells (220 HO states). The two body kinetic energy correction has been fully taken into account in the variational process. The Coulomb exchange part of the interaction has not been included into the variational process but added, in a perturbative fashion, at the end of the calculation. Reflection symmetry has been used as a selfconsistent symmetry in our HFB wave functions. This is not a real limitation as octupole instability is expected [3] at much higher spins than the ones considered in this work.

The operator

$$\hat{P}_{00}^I = \frac{2I+1}{8\pi^2} \int d\Omega d_{00}^I(\beta) e^{-i\alpha J_z} e^{-i\beta J_y} e^{-i\gamma J_z} \quad (2)$$

appearing in Eq. (1) is the usual angular momentum projector with the $K = 0$ restriction [17] and $f_\sigma^I(q_{20})$ are the ‘‘collective wave functions’’ solution of the Hill-Wheeler (HW) equation

$$\int dq_{20}' \mathcal{H}^I(q_{20}, q_{20}') f_\sigma^I(q_{20}') = E_\sigma^I \int dq_{20}' \mathcal{N}^I(q_{20}, q_{20}') f_\sigma^I(q_{20}'). \quad (3)$$

In the HW equation we have introduced the projected norm $\mathcal{N}^I(q_{20}, q_{20}') = \langle\varphi(q_{20})|\hat{P}_{00}^I|\varphi(q_{20}')\rangle$, and the projected hamiltonian kernel $\mathcal{H}^I(q_{20}, q_{20}') = \langle\varphi(q_{20})|\hat{H}\hat{P}_{00}^I|\varphi(q_{20}')\rangle$.

The solution of the HW equation for each value of the angular momentum I determines not only the ground state ($\sigma = 1$), which is a member of the Yrast band, but also excited states ($\sigma = 2, 3, \dots$) that, in the present context, may correspond to states with different deformation than the ground state and/or quadrupole vibrational excitations. In order to solve the HW equation it is usually convenient to work in an orthogonal basis given by the states $|k^I\rangle = (n_k^I)^{-1/2} \int dq_{20} u_k^I(q_{20}) \hat{P}_{00}^I |\varphi(q_{20})\rangle$ defined in terms of the quantities $u_k^I(q_{20})$ and n_k^I which are eigenvectors and eigenvalues, respectively, of the projected norm, i.e. $\int dq_{20}' \mathcal{N}^I(q_{20}, q_{20}') u_k^I(q_{20}') = n_k^I u_k^I(q_{20})$. The correlated wave functions are written in terms of the new basis as $|\Phi_\sigma^I\rangle = \sum_k g_k^{\sigma, I} |k^I\rangle$ where the amplitudes $g_k^{\sigma, I}$ have been introduced. In terms of these amplitudes it is possible to define ‘‘collective’’ wave functions $g^{\sigma, I}(q_{20}) = \sum_k g_k^{\sigma, I} u_k^I(q_{20})$ whose square, contrary to the $f_\sigma^I(q_{20})$ amplitudes, has the meaning of a probability. In the solution of the HW equation a technical difficulty is encountered: for q_{20} values close to sphericity and $I \neq 0$, the projected norms $\mathcal{N}^I(q_{20}, q_{20}')$ get very small and, as a consequence, the evaluation of the hamiltonian kernels for those values of q_{20}, q_{20}' and I is prone to strong numerical instabilities. The most notorious consequence is that the angular momentum projected (AMP) energy $E^I(q_{20}) = \mathcal{H}^I(q_{20}, q_{20})/\mathcal{N}^I(q_{20}, q_{20})$ can not be accurately computed for q_{20} close to sphericity and $I \neq 0$. For this reason, whenever the AMP energies are plotted in the next section the values corresponding to q_{20} near sphericity will be omitted. However, this difficulty does not pose any problem for the solution of the HW equation because the configurations with very small projected norms only contribute to the orthogonal states $|k^I\rangle$ with very small values of n_k^I and these states are not taken into account in the solution of the HW equation. Let us also mention that details pertaining the evaluation of the hamiltonian kernels for density dependent forces are given in [18,19].

Finally, it has to be said that one of the drawbacks of the method is that the intrinsic wave functions are determined before the projection, i.e. we are using a Projection After Variation (PAV) method. A better way to proceed would be to use Projection Before the Variation (PBV) [20] but this would lead us to a triaxial projection which, for the moment, is extremely costly for the full configuration spaces used with the Gogny force (see [21] for an implementation of PBV in small configuration spaces). According to the results of refs. [22,23] the PBV energy for strongly deformed systems (computed after several approximations) can be written as $E_{PBV}(I) = \langle H \rangle - \frac{\langle \mathcal{J}_Y^2 \rangle}{2\mathcal{J}_Y} + \frac{\hbar^2 I(I+1)}{2\mathcal{J}_{TV}}$ where \mathcal{J}_Y and \mathcal{J}_{TV} are the Yoccoz (Y) and Thouless-Valatin (TV) moments of inertia, respectively. For the PAV one has to replace the TV moment of inertia by the Y one in the last term of the previous formula. These results mean that the rotational energy correction at $I = 0$ is already well described in the PAV but for $I \neq 0$ one has to use the PBV method. As discussed in [19] the effect of the PBV can be estimated by carrying out Self Consistent Cranking (SCC) calculations. When the results of these calculations are compared to those of the AMP in several Mg isotopes it is found that the SCC gamma ray energies are quenched by a factor 0.7 with respect to the AMP ones. As we will see in the next section the same quenching factor appears for the SD rotational band when the SCC and the AMP results are compared.

III. DISCUSSION OF THE RESULTS.

In Figure 1 we present the results of the HFB calculations used to generate the intrinsic states $|\varphi(q_{20})\rangle$. On the left hand side of the figure we show the HFB energy (lower panel) along with the β_4 deformation parameter (middle panel) and the particle-particle energy $E_{pp} = -1/2\text{Tr}(\Delta\kappa^*)$ (upper panel) for protons and neutrons as a function of the quadrupole moment q_{20} . The energy curve shows a deformed ground state minimum at $q_{20} = 0.4b$ ($\beta_2 = 0.19$) which is only 130KeV deeper than the spherical configuration. A very shallow super deformed (SD) minimum at $q_{20} = 1.9b$ ($\beta_2 = 0.73$) is also observed at an excitation energy $E_x^{HFB}(SD) = 9.85\text{MeV}$. To study the effect of the finite size of the basis in the HFB energies and in the excitation energy of the SD minimum we have carried out calculations including 18 major shells for the HO basis¹ (1140 states) for both the normal deformed (ND) and SD HFB minima and found that the corresponding energies are shifted downwards by 759KeV and 1071KeV respectively. As a consequence, the excitation energy of the SD minimum gets reduced by 312KeV (a 4% effect) up to the value $E_x^{HFB}(SD) = 9.54\text{MeV}$. The hexadecupole deformation parameter β_4 is seen to increase with increasing quadrupole moments and reach at the SD minimum the rather high value $\beta_4 = 0.33$. Concerning the particle-particle correlation energies E_{pp} we observe that their values for protons and neutrons are nearly identical and they go to zero in both the normal deformed and superdeformed minima. This implies that dynamical pairing effects could be relevant for the description of both the ND and SD bands. On the right hand side of the figure we have plotted the matter density contour plots (at a density $\rho_0 = 0.08\text{fm}^{-3}$) for several values of q_{20} . Only for q_{20} values greater or equal $3.2b$ the matter density distribution resembles the one corresponding to two touching ^{16}O spherical nuclei. On the other hand, the matter distribution corresponding to the SD minimum ($q_{20} = 2b$) resembles closely the density obtained in the two-center harmonic oscillator model by coalescing (i.e. taking the distance between the centers of the two harmonic oscillator potentials equal to zero) the configuration corresponding to two separate ^{16}O nuclei in their ground states (see [5] and references therein). In this case and according to the Harvey prescription the resulting ^{32}S nucleus is not formed in its ground state but rather in the excited configuration $(0)^4(1)^{12}(2)^{12}(3)^4$ where four particles have been promoted from the $N = 2$ major shell to the $N = 3$ one. According to the ideas developed by Rae [24] relating clustering to the appearance of shell gaps in the single particle spectrum the above configuration correspond to a deformed nucleus with an axis ratio of $2 : 1$. In fact, the matter distribution of the SD minimum has an axis ratio $z/x = 1.92$, a proton mean square radius of 3.66fm and deformation parameters $\beta_2 = 0.73$ and $\beta_4 = 0.33$. To study further the connection between these ideas and our HFB results for the SD minimum we have computed the spherical shell occupancies $\nu(nlj) = \sum_m \langle \varphi | c_{nljm}^\dagger c_{nljm} | \varphi \rangle$ for the intrinsic SD wave function. The quantities $\nu(nlj)$ give the occupancy (or contents) of the HO orbital nlj in the intrinsic wave function $|\varphi\rangle$. The positive parity level occupancies are 3.168, 1.688 and 0.706 for the $d_{5/2}$, $d_{3/2}$ and $2s_{1/2}$ orbitals respectively whereas for the negative parity levels the occupancies are 0.992, 0.282, 0.864 and 0.174 for the $1f_{7/2}$, $1f_{5/2}$, $2p_{3/2}$ and $2p_{1/2}$ orbitals respectively (the quantities for proton and neutrons are very similar and therefore only the proton values are given). Therefore we have for the SD intrinsic state 11.124 particles in the $N = 2$ major shell and 4.624 in the $N = 3$ one in good agreement with the Harvey prescription. As a consequence of these occupancies, we get contributions to the quadrupole moment both from the positive parity (sd) orbitals and the negative parity (pf) ones. The two contributions turn out to be nearly the same for the SD intrinsic wave function. These values of the occupancies also imply that for a proper description of the SD configuration in terms of the shell model one needs to consider not only the sd shell but also the complete fp shell. Finally, let us mention that the occupancies of the negative parity orbitals just mentioned are very small for the ND minimum as expected.

On the left hand side of Figure 2 we have plotted the AMP energy curves for $I = 0, \dots, 12\hbar$ (full lines) along with the HFB energy curve (dashed line) as a function of the quadrupole moment. The AMP $I = 0\hbar$ energy curve shows more pronounced ND and SD minima than the HFB one and they are located at quadrupole moments $q_{20} = 0.55b$ and $q_{20} = 2.02b$ for the ND and SD configurations. The excitation energy of the SD minimum with respect to the ground state for $I = 0\hbar$ is $E_x^{AMP}(SD) = 8.22\text{MeV}$ to be compared with the 9.85MeV obtained in the HFB calculation. Let us mention that performing the AMP calculations with 18 shells is extremely time consuming and therefore we will just use in this case the 312KeV shift obtained in the HFB to account for the effect of the finite size of the basis in the excitation energy of the SD band head. We will also use the 759KeV shift in the energy of the ground state to estimate the binding energy in the AMP-GCM calculation. If we take into consideration the 312KeV shift the excitation energy of the SD minimum in the AMP case becomes $E_x^{AMP}(SD) = 7.91\text{MeV}$ to be compared with the 9.54MeV obtained in the HFB case with 18 shells. We notice that for increasing spins, the superdeformed minimum gets more and more pronounced and becomes the ground state at spin $I = 8\hbar$. This value is four units lower than the

¹This basis is considered by some authors [2] as almost indistinguishable from an infinite basis for the nucleus considered here.

HFB predictions of [2,3]. Finally, let us mention that the main effect of considering the PBV moments of inertia (see section 2) in the AMP energy curves would be the lowering of the $I \neq 0$ curves but the $I = 0$ reference curve should remain unchanged. Therefore, we do not expect changes in our prediction of the excitation energy of the SD band head and the angular momentum for which the SD band becomes the Yrast band coming from the effects of PBV.

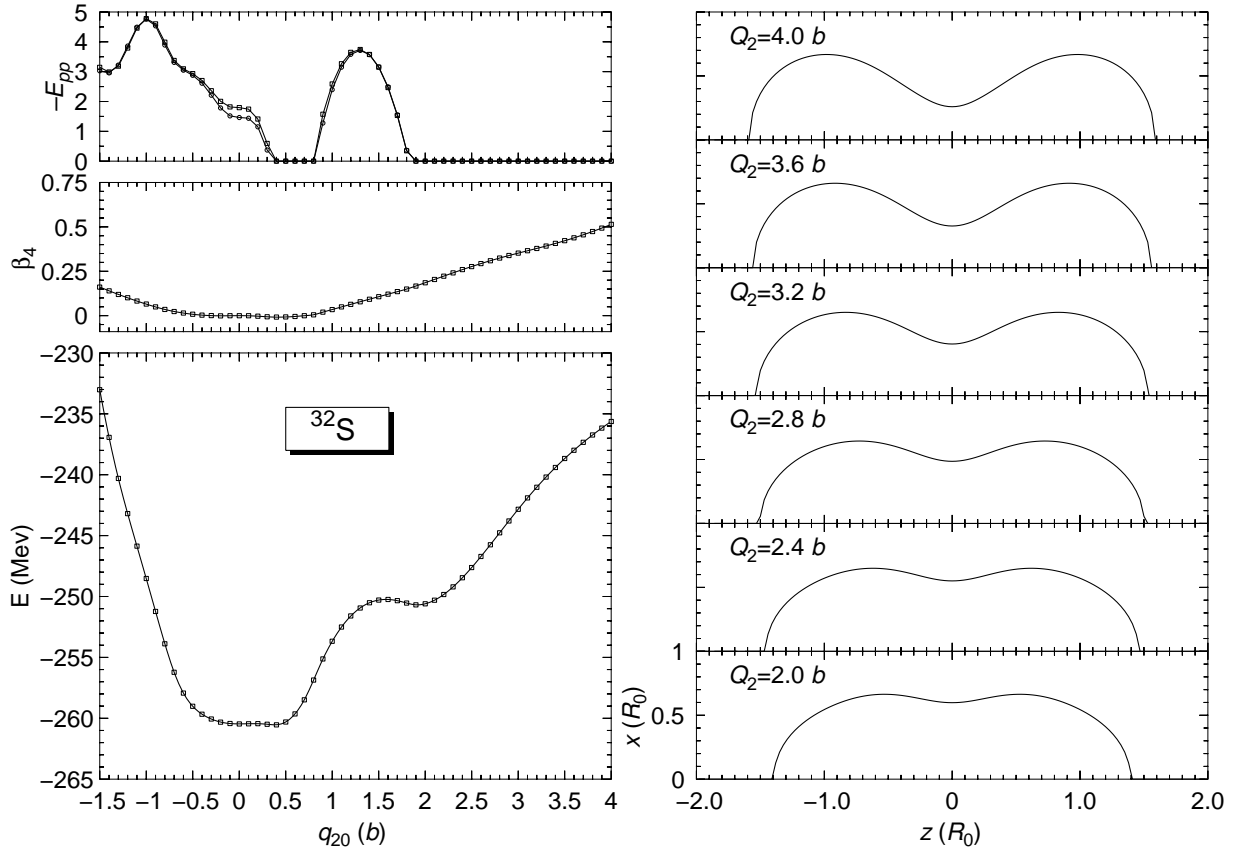


FIG. 1. On the left hand side the HFB energy (lower panel), the β_4 deformation parameter (middle panel) and the particle-particle correlation energies E_{pp} for protons and neutrons (upper panel) are depicted as a function of the quadrupole moment q_{20} given in barns. On the right hand side, contour plots of the matter distribution corresponding to a density of 0.08 fm^{-3} and different quadrupole moments are depicted.

On the right hand side of Figure 2 we show the energies obtained in the AMP-GCM calculations for the four lowest-lying solutions of the HW equation (labeled with the subindex $\sigma = 1, \dots, 4$) and spins from zero up to $12\hbar$. Each level has been placed at a q_{20} value corresponding to its average deformation $(\bar{q}_{20})^{\sigma, I} = \int dq_{20} |g^{\sigma, I}(q_{20})|^2 q_{20}$. The $I = 0\hbar$ projected energy curve has also been plotted to guide the eye.

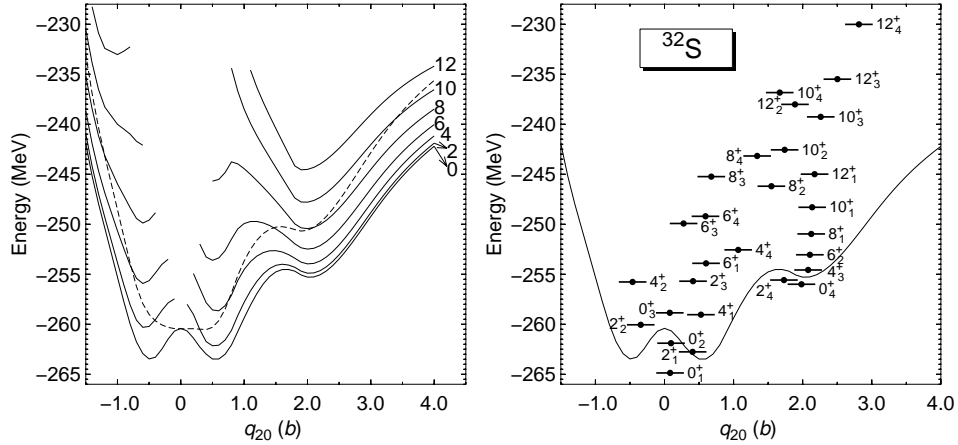


FIG. 2. In the left hand side panel the HFB energy (dashed line) and the angular momentum projected energies up to $I = 12\hbar$ are plotted as a function of the quadrupole deformation q_{20} measured in barns. See section 2 for an explanation of the missing point around $q_{20} = 0b$. In the right hand side, the four lowest-lying solutions of the AMP-GCM equation are plotted for each spin. In both plots the Coulomb exchange energy has not been added. See text for further details.

We first observe that the three lowest 0^+ states are spherical whereas the fourth one is located inside the SD minimum and therefore is the band head of the SD rotational band. As a consequence of the quadrupole mixing the excitation energy of the SD 0^+ with respect to the ground state increases up to $E_x^{AMP-GCM}(SD) = 8.87MeV$ ($8.56MeV$ for the 18 shells basis) and we also confirm that the 0^+ SD state is stable against quadrupole fluctuations. We also clearly observe the SD rotational band (0_4^+ , 2_4^+ , 4_3^+ , 6_2^+ , 8_1^+ , 10_1^+ and 12_1^+) which becomes Yrast at $I = 8\hbar$ and shows an irregularity at $I = 2\hbar$ that is related to the near degeneracy of this SD state with the 2_3^+ ND state. We also notice that a bunch of other SD states with angular momentum $10\hbar$ and $12\hbar$ appear. Let us also note that, when the Coulomb exchange energy is taken into account the 0_1^+ ground state energy becomes $-270.87MeV$ ($-271.63MeV$ when the effect of the finite size of the basis is taken into account) in good agreement with the experimental binding energy of $271.780MeV$ [25].

Concerning the normal deformed states, the 2_1^+ , 4_1^+ , 6_1^+ and 8_3^+ states have nearly the same value of $\bar{q}_{20}^{\sigma,I}$ and they could be the members of a rotational band with moderate deformation. Moreover, the 2_2^+ and 4_2^+ states are oblate and together with the 0_2^+ state could be the member of another moderate deformation band. Experimentally, there are many known levels at low excitation energy [8] either of positive and negative parity. They can be interpreted in terms of the Shell Model within the sd shell [9] or the algebraic cluster model of [10]. Some of the levels can be bunched together as members of $K = 0$ bands and could be associated to the two bands obtained in our calculations. In table 1 we compare the available experimental data on excitation energies and $B(E2)$ transition probabilities for both $K = 0$ bands with our predictions. Taking into account that in our calculations we only take into account the quadrupole degree of freedom and that the Gogny force has not been fitted for this region of the periodic table we conclude from table 1 that our results are in reasonable agreement with experiment specially for the lowest lying states. This fact gives us some confidence on the predictions we make for the SD band. In this respect, we can also mention that we obtain a spectroscopic quadrupole moment for the 2_1^+ of $-13.29fm^2$ that compares well with the experimental value [26] of $-14.9fm^2$. Our results are also in good agreement with previous calculations with the Gogny force in the context of the Bohr hamiltonian for the β and γ collective variables [15].

Band 1 (Exp)			Band 1 (Th)			Band 2 (Exp)			Band 2 (Th)		
J^π	E	$B(E2)$	J^π	E	$B(E2)$	J^π	E	$B(E2)$	J^π	E	$B(E2)$
0^+	0	-	0_1^+	0	-	0^+	3.778	-	0_2^+	2.975	-
2^+	2.230	60 ± 6	2_1^+	2.107	72.3	2^+	4.282	48.8(*)	2_2^+	4.816	58.0
4^+	4.459	72 ± 12	4_1^+	5.825	119.8	4^+	6.852	$35.4_{-8.4}^{+18.6}$	4_2^+	9.097	132.2
6^+	8.346	>22.2	6_1^+	10.962	142.8	6^+	9.783	39.6(*)	-	-	-

TABLE I. Experimental and theoretical values for the excitation energies (in MeV) and $B(E2, I \rightarrow I - 2)$ transition probabilities (in e^2fm^4) of the two $K = 0$ bands of ^{32}S . Values marked with an star correspond to theoretical predictions found in [10].

Coming back to the SD band we have also carried out SCC-HFB calculations for the SD intrinsic state to estimate the effect of PBV in the moment of inertia of the SD band (see sec. 2).

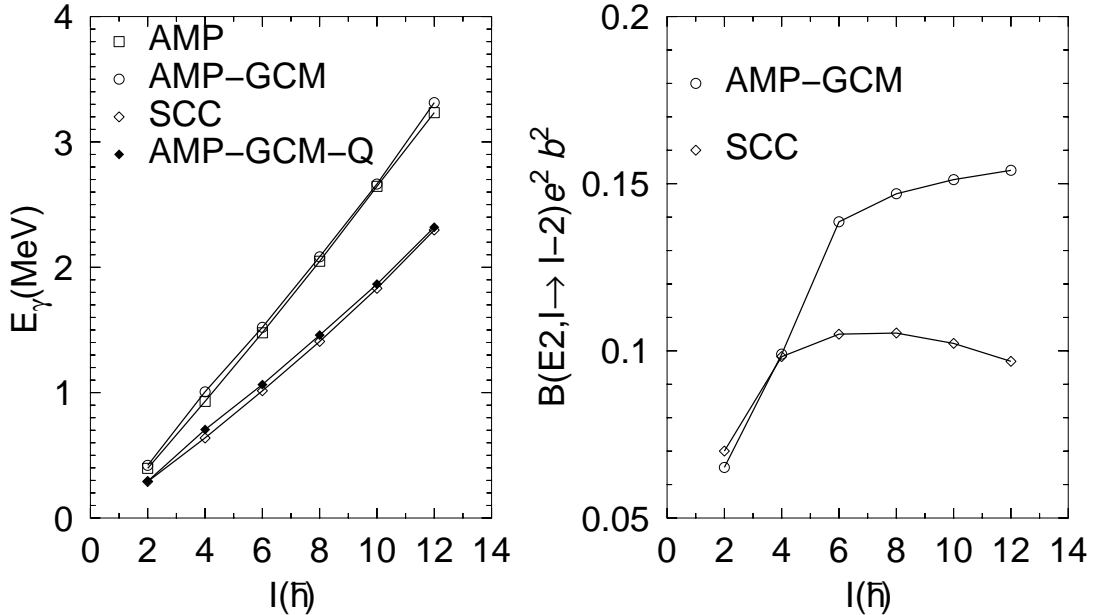


FIG. 3. On the left hand side panel the gamma ray energies $E_\gamma(I) = E(I) - E(I - 2)$ in MeV for the SD configuration are depicted as a function of spin $I(\hbar)$ for the AMP, AMP-GCM and SCC calculations. In addition, the results of the AMP-GCM quenched by a factor 0.7 (AMP-GCM-Q) are also depicted. In the right hand side panel the theoretical results for the $B(E2, I \rightarrow I - 2)$ transition probabilities in units of $e^2 b^2$ are depicted as a function of spin for the SCC and AMP-GCM calculations.

In the left panel of Figure 3 we have plotted the gamma ray energies $E_\gamma(I) = E(I) - E(I - 2)$ as a function of I for the SD band obtained with different approaches. Namely, angular momentum projection of the SD intrinsic configuration, the result of the AMP-GCM and the SCC-HFB results. We observe that the effect of the quadrupole mixing is very small as the AMP and the AMP-GCM $E_\gamma(I)$ are nearly identical. However, the SCC-HFB results are clearly different from the AMP ones. The reason was mentioned before and has to do with the fact that the moments of inertia computed in the framework of projection before (Thouless-Valatin) and after (Yoccoz) variation differ considerably. This fact has already been observed in similar calculations carried out in the same framework for several Mg isotopes [19]. In those calculations we noticed that the SCC-HFB moment of inertia turned out to be a factor 1.4 bigger than the AMP one in all the nuclei considered. The same happens here as can be seen by comparing the SCC-HFB curve with the one labeled AMP-GCM-Q which is obtained by quenching the AMP-GCM gamma ray energies by a factor 0.7. In the following we will consider the AMP-GCM-Q results for the SD rotational band as our “best” prediction. However, we have to take into account that the pairing correlations in the SD minimum are negligible and therefore one can expect that dynamic pairing could play an important role in determining the SCC moment of inertia. The static moment of inertia obtained in the AMP-GCM-Q (or the SCC-HFB) calculation is rather constant as a function of spin and has an average value of $10.3\hbar^2 MeV^{-1}$ which correspond to $k \equiv \hbar^2/(2\mathcal{J}) = 48.5 KeV$.

In the right panel of Figure 3 we show the $B(E2, I \rightarrow I - 2)$ transition probabilities along the SD band for the AMP-GCM calculation and the SCC-HFB ones computed within the rotational approximation. In both cases, the bare proton charge has been used. Both transition probabilities agree well up to $I = 6\hbar$ where the AMP-GCM results become bigger. This is related to the fact that in the SCC-HFB the Coriolis anti-stretching effect diminishes the intrinsic deformation from $\beta_2 = 0.74$ at $I = 0$ to $\beta_2 = 0.68$ at $I = 12$ whereas in the AMP-GCM the quadrupole deformation increases with spin (see the right hand side panel of Fig. 2). The Coriolis anti-stretching effect cannot be present in a AMP-GCM calculation because the intrinsic states used there are those computed at zero spin. The computed $B(E2)$ are highly collective and correspond to around $100W.u.$ for the $2^+ \rightarrow 0^+$ transition.

IV. CONCLUDING REMARKS.

As a result of our calculations we can conclude that the predicted superdeformed band in ^{32}S is stable at low spin against quadrupole fluctuations in spite of the shallowness of the HFB SD minimum. The effect of angular momentum projection and quadrupole mixing reduces the excitation energy of the SD band head with respect to the ground state to 8.87MeV (8.56MeV if the effect of the finite size basis is considered), to be compared to the HFB result of 9.85MeV (9.54MeV for the 18 shells basis). We have also found that the SD band becomes Yrast at angular momentum $I = 8\hbar$ in our calculations in contrast with the results of several HFB results where it becomes Yrast at $I = 12\hbar$. The computed moment of inertia of the SD band is of the order of $10.3\hbar^2\text{MeV}^{-1}$ and the $B(E2)$ transition probabilities along this band are very collective, exceeding $100W.u.$ The SD band head configuration corresponds to the promotion of four particles from the sd to the fp shell. As a consequence, the matter distribution of the SD configuration corresponds to two coalescent ^{16}O nuclei in the sense of the two-center harmonic oscillator shell model in good agreement with the Harvey prescription.

V. ACKNOWLEDGMENTS.

One of us (R. R.-G.) kindly acknowledges the financial support received from the Spanish Instituto de Cooperacion Iberoamericana (ICI). This work has been supported in part by the DGICyT (Spain) under project PB97/0023.

-
- [1] M. Yamagami and K. Matsuyanagi, arXiv:nucl-th/9908060.
 - [2] H. Moliq, J. Dobaczewski and J. Dudek, Phys. Rev. **C61**, 044304 (2000).
 - [3] T. Tanaka, R. G. Nazmitdinov and K. Iwasawa, arXiv:nucl-th/0004009.
 - [4] W. Nazarewicz and J. Dobaczewski, Phys. Rev. Lett. **68**, 154 (1992).
 - [5] M. Freer and A.C. Merchant, J. Phys. **G23**, 261 (1997).
 - [6] N. Curtis et al. Phys. Rev. **C53**, 1804 (1996).
 - [7] N. Cindro, Ann. Phys. (Paris) **13**, 289 (1988).
 - [8] J. Brenneisen et al. Z. Phys. **A357**, 157 (1997).
 - [9] J. Brenneisen et al. Z. Phys. **A357**, 377 (1997).
 - [10] J. Cseh, G. Lévai, A. Ventura and L. Zuffi, Phys. Rev. **C58**, 2144 (1998).
 - [11] J. Dechargé and D. Gogny, Phys. Rev. **C21**, 1568 (1980).
 - [12] J.F.Berger, M. Girod and D. Gogny, Nucl. Phys. **A428**, 23c (1984).
 - [13] H. Flocard, P.-H. Heenen, S.J. Krieger and M.S. Weiss, Prog. Theor. Phys. **72**, 1000 (1984).
 - [14] M. Girod and B. Grammaticos, Phys. Rev **C27**, 2317 (1983).
 - [15] M.C. Mermaz and M. Girod, Phys. Rev **C53**, 1819 (1996).
 - [16] F. Maréchal et al. Phys. Rev. **C60**, 034615 (1999).
 - [17] K. Hara and Y. Sun, Int. J. Mod. Phys. **E4**, 637 (1995).
 - [18] R. Rodríguez-Guzmán, J.L. Egido and L.M. Robledo, Phys. Lett. **B474**, 15 (2000).
 - [19] R. Rodríguez-Guzmán, J.L. Egido and L.M. Robledo, arXiv:nucl-th/0001020.
 - [20] P. Ring and P. Schuck, *The Nuclear Many Body Problem* (Springer, Berlin, 1980).
 - [21] K.W. Schmid and F. Grümmer, Rep. Prog. Phys. **50**, 731 (1987).
 - [22] F. Villars and N. Schmeing-Rogerson, Annals of Physics **63**, 433 (1971).
 - [23] W.A. Friedman and L. Wilets, Phys. Rev. **C2**, 892 (1970).
 - [24] W.D.M. Rae, Int. J. Mod. Phys. **A3**, 1343 (1988).
 - [25] W. Audi and A.H. Wapstra, Nucl. Phys. **A595**, 409 (1995).
 - [26] P.M. Endt, Nucl. Phys. **A510**, 1 (1990).